EUROPEAN ORGANISATION FOR NUCLEAR RESEARCH

CERN-PPE/91-86
28. May 1991

A Study of K^0_s Production in Z^0 Decays

The OPAL Collaboration

Abstract

The production of K^0 mesons in e^+e^- interactions at center of mass energies in the region of the Z^0 mass has been investigated with the OPAL detector at LEP. The rate is found to be $2.10\pm0.02\pm0.14$ $K^0, \bar{K}^0$ per hadronic event. The predictions from the JETSET and HERWIG generators agree very well with both the rate and the scale invariant cross section $1/(\sigma_{had}\beta)(d\sigma/dx_E)$ for K^0 production. Comparisons of the inclusive momentum spectrum with predictions of an analytical QCD formula and with data from lower center of mass energies are presented.

(Submitted to Physics Letters B)

The OPAL Collaboration

G. Alexander[23], J. Allison[16], P.P. Allport[5], K.J. Anderson[9], S. Arcelli[2], J.C. Armitage[6], P. Ashton[16], A. Astbury[a], D. Axen[b], G. Azuelos[18,c], G.A. Bahan[16], J.T.M. Baines[16], A.H. Ball[17], J. Banks[16], G.J. Barker[13], R.J. Barlow[16], J.R. Batley[5], G. Beaudoin[18], A. Beck[23], J. Becker[10], T. Behnke[8], K.W. Bell[20], G. Bella[23], S. Bethke[11], O. Biebel[3], U. Binder[10], I.J. Bloodworth[1], P. Bock[11], H.M. Bosch[11], S. Bougerolle[b], B.B. Brabson[12], H. Breuker[8], R.M. Brown[20], R. Brun[8], A. Buijs[8], H.J. Burckhart[8], P. Capiluppi[2], R.K. Carnegie[6], A.A. Carter[13], J.R. Carter[5], C.Y. Chang[17], D.G. Charlton[8], J.T.M. Chrin[16], P.E.L. Clarke[25], I. Cohen[23], W.J. Collins[5], J.E. Conboy[15], M. Cooper[22], M. Couch[1], M. Coupland[14], M. Cuffiani[2], S. Dado[22], G.M. Dallavalle[2], S. De Jong[8], P. Debu[21], M.M. Deninno[2], A. Dieckmann[11], M. Dittmar[4], M.S. Dixit[7], E. Duchovni[26], G. Duckeck[11], I.P. Duerdoth[16], D.J.P. Dumas[6], G. Eckerlin[11], P.A. Elcombe[5], P.G. Estabrooks[6], E. Etzion[23], F. Fabbri[2], M. Fincke-Keeler[a], H.M. Fischer[3], D.G. Fong[17], C. Fukunaga[24], A. Gaidot[21], O. Ganel[26], J.W. Gary[11], J. Gascon[18], R.F. McGowan[16], N.I. Geddes[20], C. Geich-Gimbel[3], S.W. Gensler[9], F.X. Gentit[21], G. Giacomelli[2], V. Gibson[5], W.R. Gibson[13], J.D. Gillies[20], J. Goldberg[22], M.J. Goodrick[5], W. Gorn[4], C. Grandi[2], E. Gross[26], J. Hagemann[8], G.G. Hanson[12], M. Hansroul[8], C.K. Hargrove[7], P.F. Harrison[13], J. Hart[5], P.M. Hattersley[1], M. Hauschild[8], C.M. Hawkes[8], E. Heflin[4], R.J. Hemingway[6], R.D. Heuer[8], J.C. Hill[5], S.J. Hillier[1], D.A. Hinshaw[18], C. Ho[4], J.D. Hobbs[9], P.R. Hobson[25], D. Hochman[26], B. Holl[8], R.J. Homer[1], S.R. Hou[17], C.P. Howarth[15], R.E. Hughes-Jones[16], R. Humbert[10], P. Igo-Kemenes[11], H. Ihssen[11], D.C. Imrie[25], L. Janissen[6], A. Jawahery[17], P.W. Jeffreys[20], H. Jeremie[18], M. Jimack[2], M. Jobes[1], R.W.L. Jones[13], P. Jovanovic[1], D. Karlen[6], K. Kawagoe[24], T. Kawamoto[24], R.K. Keeler[a], R.G. Kellogg[17], B.W. Kennedy[15], C. Kleinwort[8], D.E. Klem[19], T. Kobayashi[24], T.P. Kokott[3], S. Komamiya[24], L. Köpke[8], R. Kowalewski[6], H. Kreutzmann[3], J. von Krogh[11], J. Kroll[9], M. Kuwano[24], P. Kyberd[13], G.D. Lafferty[16], F. Lamarche[18], W.J. Larson[4], J.G. Layter[4], P. Le Du[21], P. Leblanc[18], A.M. Lee[17], M.H. Lehto[15], D. Lellouch[8], P. Lennert[11], C. Leroy[18], L. Lessard[18], S. Levegrün[3], L. Levinson[26], S.L. Lloyd[13], F.K. Loebinger[16], J.M. Lorah[17], B. Lorazo[18], M.J. Losty[7], X.C. Lou[12], J. Ludwig[10], M. Mannelli[8], S. Marcellini[2], G. Maringer[3], A.J. Martin[13], J.P. Martin[18], T. Mashimo[24], P. Mättig[3], U. Maur[3], T.J. McMahon[1], J.R. McNutt[25], F. Meijers[8], D. Menszner[11], F.S. Merritt[9], H. Mes[7], A. Michelini[8], R.P. Middleton[20], G. Mikenberg[26], J. Mildenberger[6], D.J. Miller[15], C. Milstene[23], R. Mir[12], W. Mohr[10], C. Moisan[18], A. Montanari[2], T. Mori[24], M.W. Moss[16], T. Mouthuy[12], P.G. Murphy[16], B. Nellen[3], H.H. Nguyen[9], M. Nozaki[24], S.W. O'Neale[8,d], B.P. O'Neill[4], F.G. Oakham[7], F. Odorici[2], M. Ogg[6], H.O. Ogren[12], H. Oh[4], C.J. Oram[e], M.J. Oreglia[9], S. Orito[24], J.P. Pansart[21], B. Panzer-Steindel[8], P. Paschievici[26], G.N. Patrick[20], S.J. Pawley[16], P. Pfister[10], J.E. Pilcher[9], J.L. Pinfold[26], D.E. Plane[8], P. Poffenberger[a], B. Poli[2], A. Pouladdej[6], E. Prebys[8], T.W. Pritchard[13], H. Przysiezniak[18], G. Quast[8], M.W. Redmond[9], D.L. Rees[1], K. Riles[4], S.A. Robins[13], D. Robinson[8], A. Rollnik[3], J.M. Roney[9], S. Rossberg[10], A.M. Rossi[2,f], P. Routenburg[6], K. Runge[10], O. Runolfsson[8], D.R. Rust[12], S. Sanghera[6], M. Sasaki[24], A.D. Schaile[10], O. Schaile[10], W. Schappert[6], P. Scharff-Hansen[8], P. Schenk[a], H. von der Schmitt[11], S. Schreiber[3], J. Schwarz[10],

J. Schwiening[3], W.G. Scott[20], M. Settles[12], B.C. Shen[4], P. Sherwood[15], R. Shypit[b], A. Simon[3], P. Singh[13], G.P. Siroli[2], A. Skuja[17], A.M. Smith[8], T.J. Smith[8], G.A. Snow[17], R. Sobie[g], R.W. Springer[17], M. Sproston[20], K. Stephens[16], H.E. Stier[10], D. Strom[9], H. Takeda[24], T. Takeshita[24], P. Taras[18], S. Tarem[26], P. Teixeira-Dias[11], N.J. Thackray[1], T. Tsukamoto[24], M.F. Turner[5], G. Tysarczyk-Niemeyer[11], D. Van den plas[18], R. Van Kooten[8], G.J. VanDalen[4], G. Vasseur[21], C.J. Virtue[19], A. Wagner[11], C. Wahl[10], J.P. Walker[1], C.P. Ward[5], D.R. Ward[5], P.M. Watkins[1], A.T. Watson[1], N.K. Watson[8], M. Weber[11], S. Weisz[8], P.S. Wells[8], N. Wermes[11], M. Weymann[8], M.A. Whalley[1], G.W. Wilson[21], J.A. Wilson[1], I. Wingerter[8], V-H. Winterer[10], N.C. Wood[16], S. Wotton[8], T.R. Wyatt[16], R. Yaari[26], Y. Yang[4,h], G. Yekutieli[26], I. Zacharov[8], W. Zeuner[8], G.T. Zorn[17].

[1]School of Physics and Space Research, University of Birmingham, Birmingham, B15 2TT, UK
[2]Dipartimento di Fisica dell' Università di Bologna and INFN, Bologna, 40126, Italy
[3]Physikalisches Institut, Universität Bonn, D-5300 Bonn 1, FRG
[4]Department of Physics, University of California, Riverside, CA 92521 USA
[5]Cavendish Laboratory, Cambridge, CB3 0HE, UK
[6]Carleton University, Dept of Physics, Colonel By Drive, Ottawa, Ontario K1S 5B6, Canada
[7]Centre for Research in Particle Physics, Carleton University, Ottawa, Ontario K1S 5B6, Canada
[8]CERN, European Organisation for Particle Physics, 1211 Geneva 23, Switzerland
[9]Enrico Fermi Institute and Department of Physics, University of Chicago, Chicago Illinois 60637, USA
[10]Fakultät für Physik, Albert Ludwigs Universität, D-7800 Freiburg, FRG
[11]Physikalisches Institut, Universität Heidelberg, Heidelberg, FRG
[12]Indiana University, Dept of Physics, Swain Hall West 117, Bloomington, Indiana 47405, USA
[13]Queen Mary and Westfield College, University of London, London, E1 4NS, UK
[14]Birkbeck College, London, WC1E 7HV, UK
[15]University College London, London, WC1E 6BT, UK
[16]Department of Physics, Schuster Laboratory, The University, Manchester, M13 9PL, UK
[17]Department of Physics and Astronomy, University of Maryland, College Park, Maryland 20742, USA
[18]Laboratoire de Physique Nucléaire, Université de Montréal, Montréal, Quebec, H3C 3J7, Canada
[19]National Research Council of Canada, Herzberg Institute of Astrophysics, Ottawa, Ontario K1A 0R6, Canada
[20]Rutherford Appleton Laboratory, Chilton, Didcot, Oxfordshire, OX11 0QX, UK
[21]DPhPE, CEN Saclay, F-91191 Gif-sur-Yvette, France
[22]Department of Physics, Technion-Israel Institute of Technology, Haifa 32000, Israel
[23]Department of Physics and Astronomy, Tel Aviv University, Tel Aviv 69978, Israel

[24]International Centre for Elementary Particle Physics and Dept of Physics, University of Tokyo, Tokyo 113, and Kobe University, Kobe 657, Japan
[25]Brunel University, Uxbridge, Middlesex, UB8 3PH UK
[26]Nuclear Physics Department, Weizmann Institute of Science, Rehovot, 76100, Israel

[a]University of Victoria, Dept of Physics, P O Box 3055, Victoria BC V8W 3P6, Canada
[b]University of British Columbia, Dept of Physics, 6224 Agriculture Road, Vancouver BC V6T 1Z1, Canada
[c]Also at TRIUMF, Vancouver, Canada V6T 2A3
[d]On leave from Birmingham University, Birmingham B15 2TT, UK
[e]Univ of Victoria, Dept of Physics, P.O. Box 1700, Victoria BC V8W 2Y2, Canada and TRIUMF, Vancouver, Canada V6T 2A3
[f]Present address: Dipartimento di Fisica, Università della Calabria and INFN, 87036 Rende, Italy
[g]University of British Columbia, Dept of Physics, 6224 Agriculture Road, Vancouver BC V6T 2A6, Canada and IPP, McGill University, High Energy Physics Department, 3600 University Str, Montreal, Quebec H3A 2T8, Canada
[h]On leave from Research Institute for Computer Peripherals, Hangzhou, China

Introduction

In this paper, the first measurement of the process $e^+e^- \to \mathrm{K}^0_s X$ at $\sqrt{s} \simeq M_{Z^0}$ is presented. The results have been obtained with the OPAL detector at the CERN LEP collider. K^0_s mesons were identified in the decay channel $\mathrm{K}^0_s \to \pi^+\pi^-$ by reconstruction of the decay vertex and the invariant mass of the decay system.

Hadron production in e^+e^- interactions involves the fragmentation process, the transition of coloured partons into colourless hadrons. No exact theoretical prescription exists for this process yet. Rather, a variety of phenomenological models has been developed. At present, the most commonly used ones are the string fragmentation model [1] and the cluster fragmentation model [2]. Strange particle production in e^+e^- annihilations [3][4][5] has been an important tool in studying the fragmentation process, since K^0_s mesons can be cleanly identified over a large momentum range. We compare the measured K^0 momentum spectrum with predictions of the JETSET [6] and HERWIG [7] models and find that the total K^0 rate and the differential cross section are in good agreement with both models.

Another approach to describe the hadron momentum spectra combines the modified leading log approximation (MLLA) [8] of QCD with the picture of local parton hadron duality (LPHD) [8]. The MLLA approximation consists of a summation of double and single leading–log contributions. It predicts the momentum spectrum of partons. The LPHD hypothesis assumes that the measured hadron spectra can be directly compared to the calculated parton spectra. Our measurement is compared with an analytical formula derived within the MLLA and LPHD framework.

Finally, a comparison of our data with experimental results from lower energies is presented, showing the evolution of the K^0 multiplicity as well as the behaviour of the differential cross section as a function of the center of mass energy.

The OPAL Detector and Hadronic Event Selection

The OPAL detector, a multi–purpose detector designed to reconstruct the decay products of the Z^0 Boson, has been described in detail elsewhere [9]. The present analysis is based mainly on the information from the central tracking chambers, consisting of a large jet chamber, a precision vertex detector and additional z-chambers surrounding the jet chamber. The main detector, the jet chamber, has a length of 4 m and a diameter of 3.7 m. It is divided into 24 sectors, each equipped with 159 sense wires ensuring a large number of measured points even for particles emerging from a secondary vertex. The vertex detector, a 1 m long cylindrical drift chamber of 470 mm diameter, surrounds the beam pipe and consists of an inner layer of 36 cells each with 12 sense wires and an outer layer of 36 small angle (4°) stereo cells each with 6 sense wires. The z-chambers consist of 24 drift chambers, 4 m long, 50 cm wide and 59 mm thick. They are subdivided in 8 cells each with 6 sense wires perpendicular to those of the jet chamber. They cover a polar angle from 44° to 136° and 94% of the azimuthal angle. All the chambers are contained in a solenoid providing an axial magnetic field of 0.435

T.

The present analysis was performed on 144473 hadronic decays of the Z^0 recorded during 1990 at center-of-mass energies between 88.2 and 94.3 GeV with a luminosity-weighted average energy of 91.31 GeV. The selection of the hadronic event sample relying on the information of the electromagnetic calorimeter and the time-of-flight counters has been described elsewhere [10]. In addition each event was required to have at least five well reconstructed charged tracks.

The K_s^0 Finding Algorithm

The search for K_s^0 was performed via the decay into $\pi^+\pi^-$ by systematically pairing oppositely charged tracks.

Each track had to fulfill the following conditions: A minimum transverse momentum with respect to the beam direction of 150 MeV/c, at least 80 jet chamber hits and at least 4 z-chamber hits were required; the latter to ensure a good mass resolution by improving the measurement of the polar angle. Due to the geometrical acceptance of the z-chambers, this restricts the range of the polar angle with respect to the beam direction to $|\cos\theta| < 0.7$. Furthermore, the radial distance of the track to the beam axis at the point of closest approach was required to exceed 3 mm to reduce the large combinatorial background.

Intersection points of track pairs in the radial plane were considered to be candidate secondary vertices. Additional cuts were imposed on these pairs: The radial distance from the intersection point to the primary vertex had to be larger than 1 cm and the reconstructed momentum vector of the K_s^0 candidate in the plane perpendicular to the beam had to point to the beam axis within 2°. In the case where both intersections of the track pair passed these cuts, the one closer to the beam axis was taken.

Finally, all track pairs which had passed the cuts were refit with the constraint to originate from a common 3-dimensional vertex. Pairs with an invariant mass of less than 100 MeV/c^2 (assuming both tracks to be electrons) were considered to be photon conversions and rejected.

After applying this procedure to the hadronic event sample and assigning the pion mass to both tracks, the mass distribution shown in Fig. 1a was obtained. A fit with a Gaussian for the signal plus a third order polynomial background describes the spectrum well and yields $m_{K_s^0}$=497.2 $\pm$ 0.1 MeV/c^2 and σ=6.5 $\pm$ 0.1 MeV/c^2 in reasonable agreement[1] with the PDG [11] value of 497.7 MeV/c^2 and the expected mass resolution from a Monte Carlo simulation of the OPAL detector, respectively. The peak contains 13816 $\pm$ 118 K_s^0 (statistical error only).

[1]The given error is statistical only; the remaining difference can be explained by the uncertainty in the mean value of the magnetic field

Differential and Integrated Cross Sections

In order to extract the number of K_s^0 and thus to determine the K_s^0 cross section, it is neccessary to estimate the amount of background under the signal peak and to correct for the detection efficiency. For this purpose, fits similar to those described above were performed in different K_s^0 momentum bins. To determine the number of K_s^0 per momentum bin, the entries in the mass range from 450 MeV/c^2 to 550 MeV/c^2 were summed up and the background obtained from the fitted polynomial function was subtracted. This was followed by an efficiency correction performed separately in each momentum bin. The detection efficiency defined as $\epsilon = n^{K_s^0}_{reconstructed}/n^{K_s^0}_{generated}$ was calculated using a sample of Monte Carlo events that were passed through a detailed simulation of the OPAL detector and subjected to the same analysis chain as the real data.

The agreement between real data and simulated data was checked and in general found to be good, although it was observed that the fraction of charged tracks having at least 4 z-chamber hits is 82.2% in the data compared to 90.3% in the detector simulation. This effect is due to an incorrect estimation of the jet chamber z resolution and of the z–chamber sensitive volume in the simulation. The detection efficiency has been corrected for this difference on a track by track basis.

Fig. 1b shows the resulting detection efficiency for $K_s^0 \to \pi^+\pi^-$ as a function of the K_s^0 momentum obtained with a hadronic event sample generated with the JETSET Monte Carlo. It shows a maximum of 27 % at a momentum of about 3 GeV/c. At high momenta, the efficiency is mainly limited by the requirement of 80 jet chamber hits which cannot be met by K_s^0 decaying too far from the beam axis. Apart from the track cut at small transverse momentum, the decrease at low momentum is mainly due to the cut on the radial distance from the intersection point to the primary vertex.

To estimate the uncertainty of the detection efficiency, the same calculation was repeated using events produced with the HERWIG generator. In addition, the K_s^0 selection cuts were varied. From these studies, we determined the detection efficiency uncertainty to be about 5 %. It enters as an overall normalization error into the systematic error of our measurement. As further sources of possible systematic errors we considered the following two contributions: An uncertainty in the matching to the z–chamber was accounted for by including an error of 3 % in the overall normalization error, which brings it up to 6 % in total. The uncertainty in the background subtraction described above was determined by varying the fit range and the background shape. It was estimated to be about 7 % entering as a bin–to–bin uncertainty; this then contributes 3 % to the uncertainty of the total rate by quadratic addition of the contributions from all momentum bins. In total, the systematic uncertainty of the integrated K^0 rate was found to be 7 % after combining all these effects.

After correcting the data for the unobserved decay into $\pi^0\pi^0$ and for K_L^0 production, the scale invariant cross section $1/(\sigma_{had}\beta)(d\sigma/dx_E)$ for K^0 production[2] was obtained as a function of the scaled energy $x_E = 2E_{K^0}/\sqrt{s}$. It is shown in Fig. 2 and Table 1.

[2]By denoting the particle state we mean both particle and antiparticle state

The indicated error bars include statistical and bin–to–bin systematic contributions. In addition there is an overall normalization uncertainty of 6 % mentioned above.

The predictions of the JETSET 7.2 and HERWIG 5.0 generators are also shown in Fig. 2 along with our data. The fragmentation parameters of these programs were tuned to describe the global event shapes as measured by OPAL[3] [12]. Whenever refering to the generators throughout this paper, we use these tuned versions. The predictions of both generators are very similar; they exhibit good agreement with the measurements.

To determine the total K^0 rate, the momentum spectrum was integrated, using JETSET to extrapolate over the unobserved momentum region; the size of this correction was 5%. $2.10 \pm 0.02 \pm 0.14$ K^0 per hadronic event were found. The first error quoted is statistical while the second reflects the systematic uncertainties.

Adjusting the γ_s parameter in JETSET which controls the suppression of s quark pair production in the colour field to describe the measured cross section yields $\gamma_s = 0.285 \pm 0.035$. The other model parameters were kept fixed. Our measurement is consistent with the default value $\gamma_s = 0.3$ which has been determined with data from lower center of mass energies, indicating the independence of γ_s on the center of mass energy. For example, the JADE collaboration measured a value of $\gamma_s = 0.27 \pm 0.03 \pm 0.05$ [5], and the TASSO collaboration $\gamma_s = 0.35 \pm 0.02 \pm 0.05$ [13], respectively.

Comparison with QCD Predictions

As previously shown in [14][15] calculations for the gluon momentum spectrum in the modified leading log approximation (MLLA) [8] (see also [16]) of QCD can describe the momentum distribution of all charged particles. These calculations predict a decrease of particle yield at low momenta which is attributed to a destructive interference of coherently emitted soft gluons [17]. The agreement between the expected gluon and the observed hadron spectrum can be understood in the context of local parton–hadron duality [8]. Further insight into this matter can be gained from a comparison of the predictions for individual particle types.

Denoting $\xi = ln(1/x_p)$, where $x_p = 2c \cdot p/\sqrt{s}$ stands for the scaled momentum of the particle, the predicted hadron spectrum can be written as

$$\frac{1}{\sigma_{had}} \frac{d\sigma}{d\xi} = N \cdot f(\Lambda_{eff}, Q_0, \sqrt{s}, \xi) \,. \tag{1}$$

The theoretical predictions involve three free parameters: an effective QCD scale Λ_{eff} which is not directly related to $\Lambda_{\overline{MS}}$, a cut-off parameter in the quark–gluon cascade Q_0, and the overall normalization factor N that depends on the particle type and is expected to be independent of the center of mass energy. The predicted spectrum shows a maximum which is shifted to lower ξ values with increasing Λ_{eff}.

Comparison of the spectrum (1) with the data is not trivial since no rigorous connection between Q_0 and the particle mass is available. Instead the measurement of

[3] In HERWIG 5.0, the parameters determined to fit the event shapes as measured by OPAL are the default values

the mass dependence is hoped to provide insight into non-perturbative QCD effects. Furthermore, formula (1) is difficult to solve numerically. In [14][15], a simplified form of (1) has been applied assuming $Q_0 = \Lambda_{eff}$. This assumption is supported by the expectation that the spectrum should be insensitive to the value of Q_0 for asymptotic center of mass energies [8]. The resulting spectrum (the so–called *limiting spectrum*) is especially convenient for numerical integration. Its explicit form can be found in [18]; it is valid for $1 < \xi < ln(\sqrt{s}/2\Lambda_{eff})$. For massive hadrons, one supposes $Q_0 > \Lambda_{eff}$, and the limiting formula is expected to be less accurate [19].

In the case of all charged particles [14][15] and π^0 mesons [15] good agreement with the predicted limiting spectrum was observed. In the following we compare the measured K^0 momentum spectrum in terms of $(1/\sigma_{had})(d\sigma/d\xi)$ with the QCD calculations for $Q_0 = \Lambda_{eff}$. The measured data points are shown in Table 2 and together with the result of the fit in Fig. 3. The fit range was restricted to $|\xi - \xi_{max}| < 1$ around the position of the maximum ξ_{max}. There is good agreement in the range included in the fit; the data points in the low ξ region are also reasonably described by the prediction. However, the data show a general tendency towards a broader distribution. For the free parameters of the fit we obtain $\Lambda_{eff} = 827 \pm 30$ MeV and $N = 0.211 \pm 0.003$. The errors of the parameters were determined by varying the K^0_s selection cuts and the range of data points included in the fit. We find the position of the maximum at $\xi^{K^0}_{max} = 2.91 \pm 0.04$. Compared to the values obtained for all charged particles of $\xi^{charged}_{max} = 3.603 \pm 0.013$ [14], $\xi^{charged}_{max} = 3.71 \pm 0.05$ [15], and for π^0 mesons of $\xi^{\pi^0}_{max} = 4.11 \pm 0.18$ [15], we find that for the more massive K^0 the position of the maximum is shifted to lower values of ξ. This trend of the maximum position decreasing with increasing particle mass has already been observed at lower center of mass energies by the TASSO collaboration [20]. Corresponding to the shift of the maximum, the limiting formula yields for the K^0 a value of Λ_{eff} considerably higher than for the light mesons ($\Lambda^{charged}_{eff} = 253 \pm 30$ MeV [14], $\Lambda^{charged}_{eff} = 220 \pm 20$ MeV [15] and $\Lambda^{\pi^0}_{eff} = 115 \pm 40$ MeV [15]). The strong dependence of Λ_{eff} on the particle mass is expected to be due to mass effects which are not taken into account in the context of the limiting formula.

A more natural description of the spectra of massive mesons is expected using the full equation (1) instead of the limiting spectrum. The same value of Λ_{eff} is supposed to describe the spectra of light and heavy hadrons, whereas Q_0 should be related to the particle mass. In a recent paper [21], a method to solve (1) approximately has been proposed and a spectrum for Λ_{eff}=150 MeV, Q_0=300 MeV is presented as illustration. The value of Λ_{eff} was chosen to be consistent with the measurements of the light mesons. This spectrum, normalized to our data, is plotted as the dashed line in fig 3. Although no fit to determine the parameters was performed, a reasonable description of the measured data points is found, supporting the above mentioned expectation of a unique value of Λ_{eff} for light and heavy mesons and Q_0 increasing with the particle mass.

Comparison with Data from Different Center of Mass Energies

Fig. 4a shows the number of K^0 per hadronic event determined by different experiments [3][4][5] in a range of center of mass energy from 12 to 91 GeV. The numbers from lower energies stem from a compilation recently published by the TASSO collaboration [4]. In Table 3 the predictions for the K^0 multiplicity of JETSET and HERWIG[4] at $\sqrt{s} = 35$ GeV and $\sqrt{s} = 91$ GeV are compared with experimental data. The measured K^0 multiplicities are well described at both center of mass energies.

Fig. 4b shows the scaling cross section $1/(\sigma_{had}\beta)(d\sigma/dx_E)$ as a function of the center of mass energy in various x_E bins as measured by OPAL, TASSO and TPC. The evolution of the cross section with the center of mass energy is influenced by two effects: On one hand, scaling violations which are due to gluon emission can be expected. They would lead to a decrease of the cross section at high x_E values and to a corresponding increase at low values of x_E. On the other hand, electroweak effects become important if the center of mass energy approaches the Z^0 mass. In particular, the flavour composition of the primary produced quarks is different due to the different couplings to photon and Z^0 respectively.

The solid line in Fig. 4b shows the JETSET prediction for the energy evolution of the K^0 cross section including electroweak effects; the dashed line shows the behaviour with pure photon exchange, demonstrating the influence of scaling violations. The full curve exhibits a rise of the cross section compared to the photon exchange case especially at large x_E. This is due to the larger coupling of down–type quarks to the Z^0 , resulting in a larger fraction of primary strange quarks which yields more strange mesons with high momenta.

Summary

The differential and total cross sections for K^0 production in e^+e^- annihilation at $\sqrt{s} \simeq M_{Z^0}$ have been measured from 144473 hadronic events recorded with the OPAL detector in 1990. The yield was found to be $2.10 \pm 0.02 \pm 0.14$ K^0 per event. The total rate as well as the differential cross section with respect to momentum as predicted by JETSET and HERWIG are in good agreement with the data. Furthermore, the evolution of the K^0 multiplicity with $\sqrt{s}$ is well described by JETSET and HERWIG. We also compare our measurement to the predictions of analytical QCD formulae derived within the framework of the MLLA approach. A reasonable description of the spectrum is found.

[4]Also for $\sqrt{s} = 35$ GeV, the tuned parameters were used for the generators

Acknowledgements

We wish to thank Y.L. Dokshitzer and V.A. Khoze for fruitful and enjoyable discussions and correspondence.

It is a pleasure to thank the SL Division for the efficient operation of the LEP accelerator, the precise information on the absolute energy, and their continuing close cooperation with our experimental group. In addition to the support staff at our own institutions we are pleased to acknowledge the following :
Department of Energy, USA
National Science Foundation, USA
Science and Engineering Research Council, UK
Natural Sciences and Engineering Research Council,Canada
Israeli Ministry of Science
Minerva Gesellschaft
The Japanese Ministry of Education, Science and Culture (the Monbusho) and a grant under the Monbusho International Science Research Program.
American Israeli Bi-national Science Foundation.
Direction des Sciences de la Matière du Commissariat à l'Energie Atomique, France.
The Bundesministerium für Forschung und Technologie, FRG.
and The A.P. Sloan Foundation.

References

[1] B. Andersson et al., Phys. Rep. **97** (1983) 31.

[2] G.C. Fox and S. Wolfram, Nucl. Phys. **B 168** (1980) 285;
S. Wolfram, Proc. 15. Renc. de Moriond, Les Arcs 1980, 549.

[3] PLUTO Collaboration, C. Berger et al., Phys. Lett. **104 B** (1981) 79;
TPC Collaboration, H. Aihara et al., Phys. Rev. Lett. **53** (1984) 2378;
MARK II Collaboration, H. Schellman et al., Phys. Rev. **D 31** (1985) 3013;
HRS Collaboration, M. Derrick et al., Phys. Rev. **D 35** (1987) 2639;
CELLO Collaboration, H. Behrend et al., Z. Phys. **C 46** (1990) 397.

[4] TASSO Collaboration, W. Braunschweig et al., Z. Phys. **C 47** (1990) 167.

[5] JADE Collaboration, W. Bartel et al., Z. Phys. **C 20** (1983) 187.

[6] T. Sjöstrand, Comp. Phys. Comm. **39** (1986) 347;
T. Sjöstrand and M. Bengtsson, Comp. Phys. Comm. **43** (1987) 367.

[7] G. Marchesini and B.R. Webber, Nucl. Phys. **B 310** (1988) 461.

[8] Y.L. Dokshitzer and S.I. Troyan, Leningrad Preprint LNPI-922 (1984) (in Russian);
Y.I. Azimov, Y.L. Dokshitzer, V.A. Khoze and S.I. Troyan, Z. Phys. **C 27** (1985) 65.

[9] OPAL Collaboration, K. Ahmed et al., The OPAL Detector at LEP,
submitted to Nucl. Instr. and Meth.

[10] OPAL Collaboration, M.Z. Akrawy et al., Phys. Lett. **B 231** (1989) 530.

[11] Particle Data Group,
M. Aguilar–Benitez et al., Phys. Lett. **B 239** (1990).

[12] OPAL Collaboration, M.Z. Akrawy et al., Z. Phys. **C 47** (1990) 505.

[13] TASSO Collaboration, M. Althoff et al., Z. Phys. **C 27** (1985) 27.

[14] OPAL Collaboration, M. Z. Akrawy et al., Phys. Lett. **B 247** (1990) 617.

[15] L3 Collaboration, B. Adeva et al., L3 Preprint 025.

[16] A.H. Mueller, Nucl. Phys. **B213** (1983) 85;
A.H. Mueller, Nucl. Phys. **B241** (1984) 141.

[17] A.H. Mueller, Phys. Lett. **B104** (1981) 161;
A. Bassetto, M. Ciafaloni, G. Marchesini and A.H. Mueller, Nucl. Phys. **B207** (1982) 189;
B.I. Ermolaev and V.S. Fadin, JETP Lett. **33** (1981) 269;
Yu.L. Dokshitzer, V.S. Fadin, V.A. Khoze, Phys. Lett. **B115** (1982) 242.

[18] V.A. Khoze, Y.L. Dokshitzer and S.I. Troyan, Lund Preprint LU TP 90-12 (1990).

[19] V.A. Khoze, Y.L. Dokshitzer and S.I. Troyan, private communication.

[20] TASSO Collaboration, M. Althoff et al., Z. Phys. **C 22** (1984) 307.

[21] Y.L. Dokshitzer, V.A. Khoze and S.I. Troyan, Lund Preprint LU TP 91-12 (1991).

Table 1: The scaling cross section for K^0 production

x_E	$\bar{x}_E$	$\frac{1}{\sigma_{had}\beta}\frac{d\sigma}{dx_E}$
0.01-0.03	0.02	29.6 ± 2.2
0.03-0.04	0.035	21.1 ± 1.6
0.04-0.06	0.049	15.4 ± 1.1
0.06-0.10	0.078	9.0 ± 0.7
0.10-0.15	0.123	5.0 ± 0.4
0.15-0.20	0.173	2.8 ± 0.2
0.20-0.30	0.242	1.4 ± 0.1
0.30-0.40	0.343	0.75 ± 0.07
0.40-0.60	0.474	0.21 ± 0.03
0.60-1.00	0.693	0.03 ± 0.007

Table 2: The ξ distribution for K^0 production

ξ	$\frac{1}{\sigma_{had}}\frac{d\sigma}{d\xi}$
0.13 - 0.93	0.067 ± 0.009
0.93 - 1.29	0.261 ± 0.029
1.29 - 1.60	0.375 ± 0.038
1.60 - 1.80	0.463 ± 0.047
1.80 - 2.00	0.545 ± 0.055
2.00 - 2.20	0.658 ± 0.065
2.20 - 2.40	0.661 ± 0.065
2.40 - 2.60	0.726 ± 0.071
2.60 - 2.80	0.689 ± 0.067
2.80 - 3.00	0.742 ± 0.072
3.00 - 3.20	0.738 ± 0.072
3.20 - 3.40	0.649 ± 0.064
3.40 - 3.60	0.656 ± 0.065
3.60 - 3.80	0.547 ± 0.056
3.80 - 4.04	0.491 ± 0.051
4.04 - 4.33	0.472 ± 0.050
4.33 - 4.62	0.342 ± 0.043
4.62 - 5.02	0.224 ± 0.037

Table 3: K^0 multiplicity at different CMS energies compared with generator predictions

$\sqrt{s}$ [GeV]	experimental	JETSET	HERWIG
35	1.42 — 1.47	1.46	1.38
91	2.1±0.02±0.14	2.16	2.07

Figure Captions

Figure 1:
(a) Invariant mass spectrum of K^0_s candidates
(b) Detection efficiency for $K^0_s \to \pi^+\pi^-$

Figure 2:
Differential scale invariant cross section $1/(\sigma_{had}\beta)(d\sigma/dx_E)$ vs. x_E for K^0 production. The line indicates both the predictions of JETSET and HERWIG, respectively, since they can not be distinguished from each other within the line width. Indicated errors include statistical and bin–to–bin systematic contributions

Figure 3:
Measured $\xi = \ln(1/x_p)$ distribution with QCD predictions. Indicated errors include statistical and bin–to–bin systematic contributions. The dotted line shows the result of a fit using the limiting QCD formula (the solid part indicates the fit range); the dashed line illustrates an approximate solution of the full QCD formula

Figure 4:
(a) K^0 multiplicity at different center of mass energies
(b) Differential scale invariant cross section for K^0 production as a function of the squared center of mass energy in several x_E bins. The dashed line indicates the JETSET prediction for pure photon exchange, whereas the solid line shows the prediction including electroweak effects

Fig. 1a

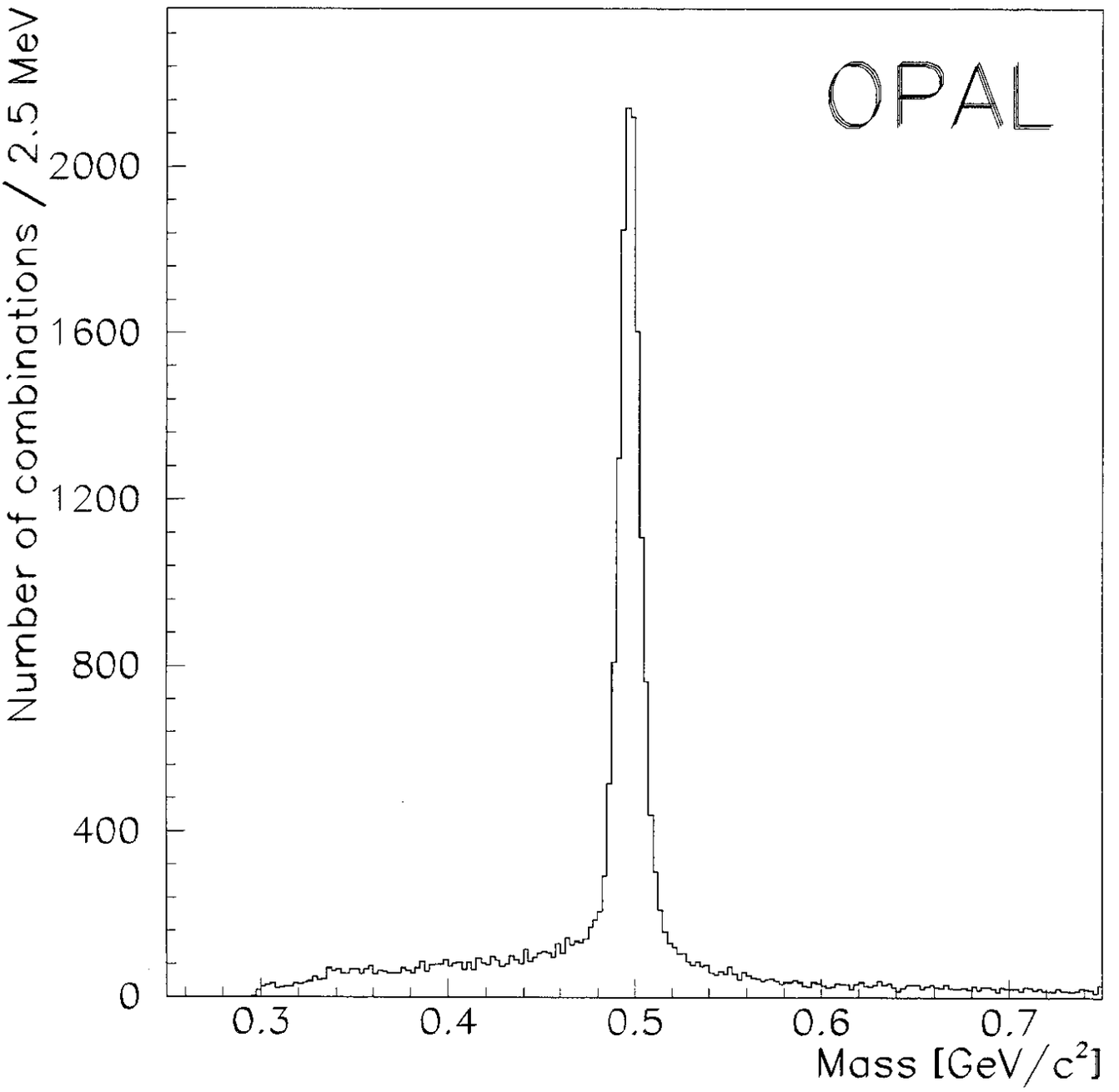
OPAL
Number of combinations / 2.5 MeV
2000
1600
1200
800
400
0
0.3
0.4
0.5
0.6
0.7
Mass [GeV/c²]

Fig. 1b

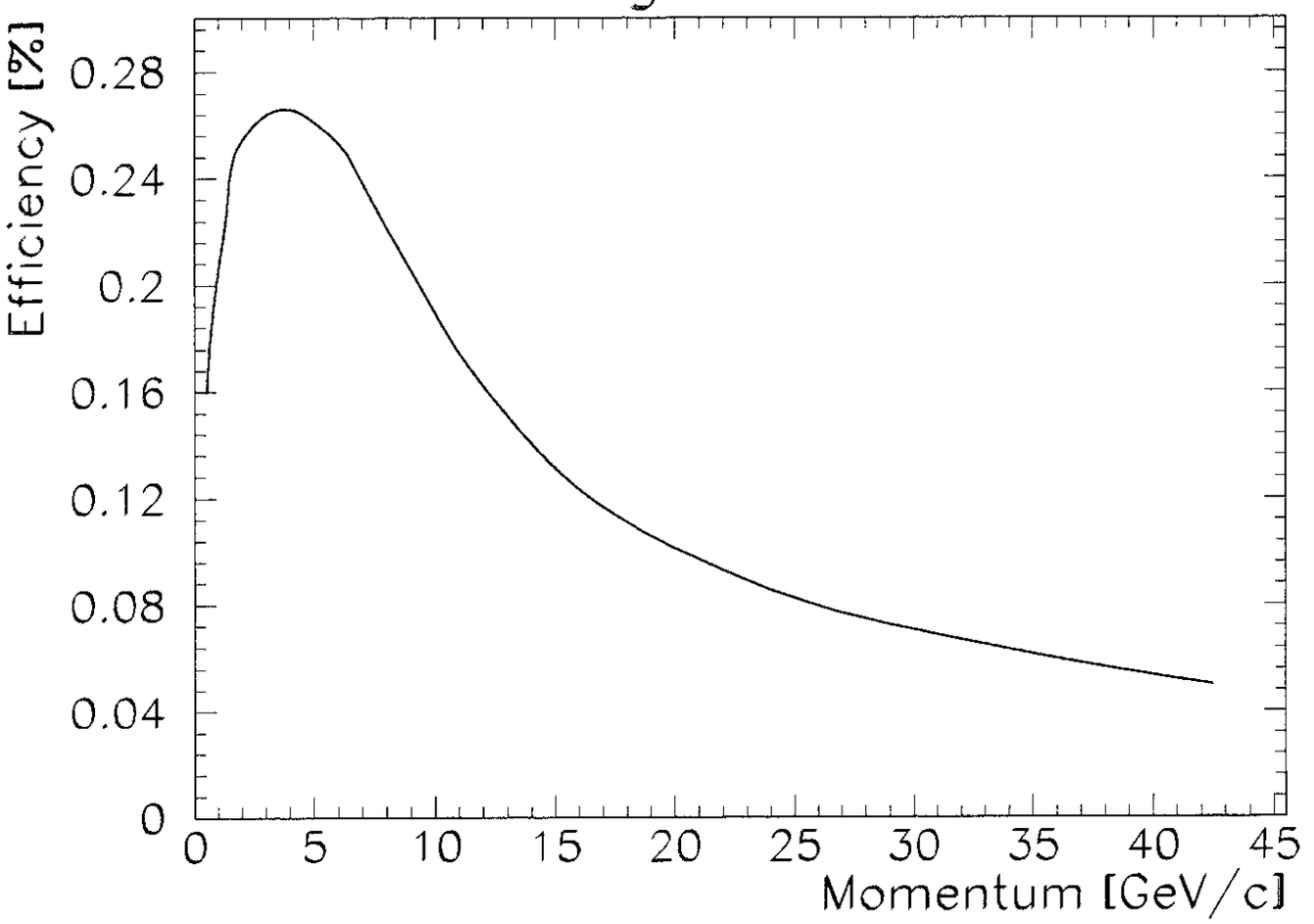
Efficiency [%]
0.28
0.24
0.2
0.16
0.12
0.08
0.04
0
0
5
10
15
20
25
30
35
40
45
Momentum [GeV/c]

Fig. 2

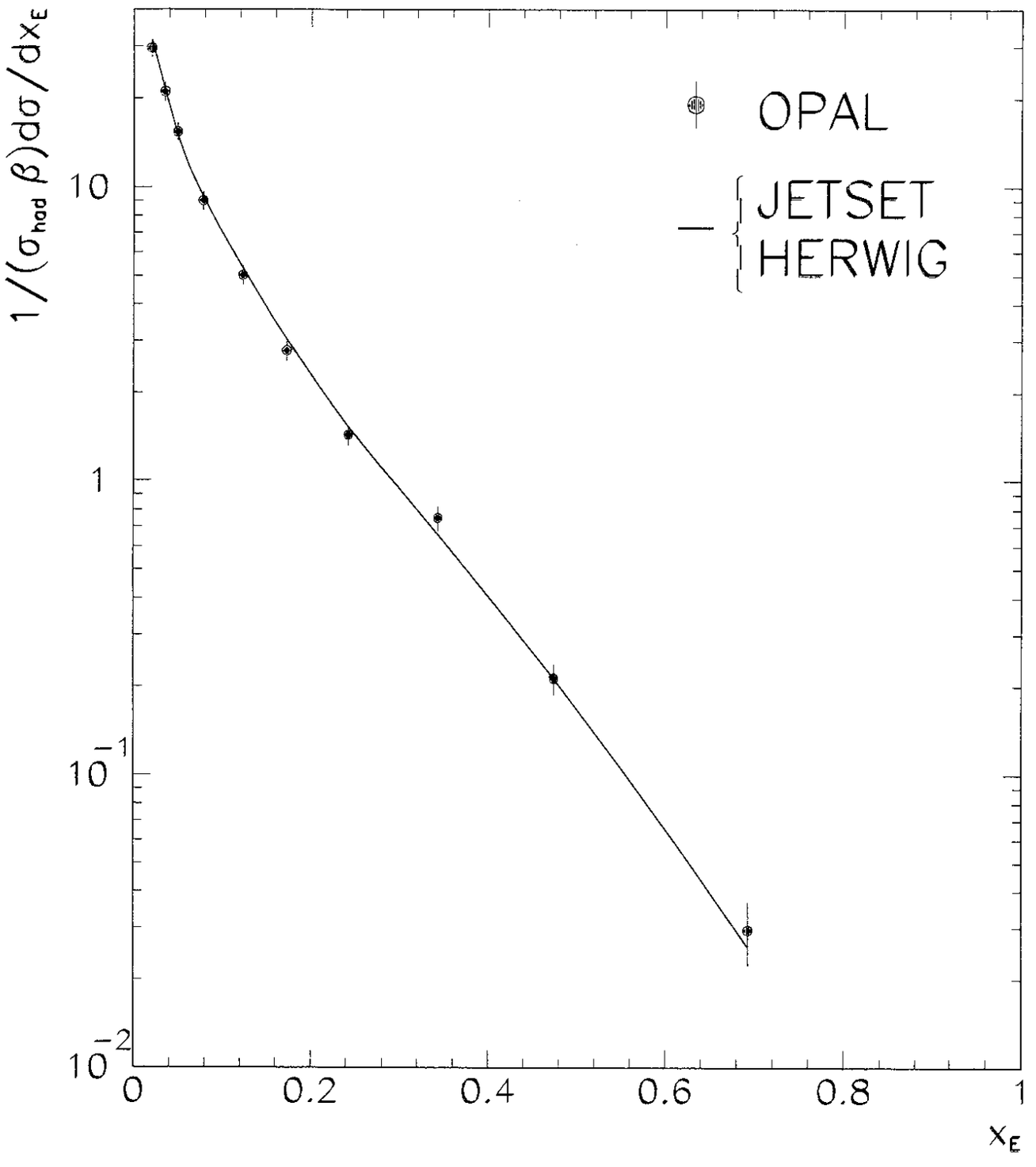
$1/(\sigma_{had}\,\beta)d\sigma/dx_E$
10
1
10^{-1}
10^{-2}
0
0.2
0.4
0.6
0.8
1
x_E
OPAL
JETSET
HERWIG

Fig. 3

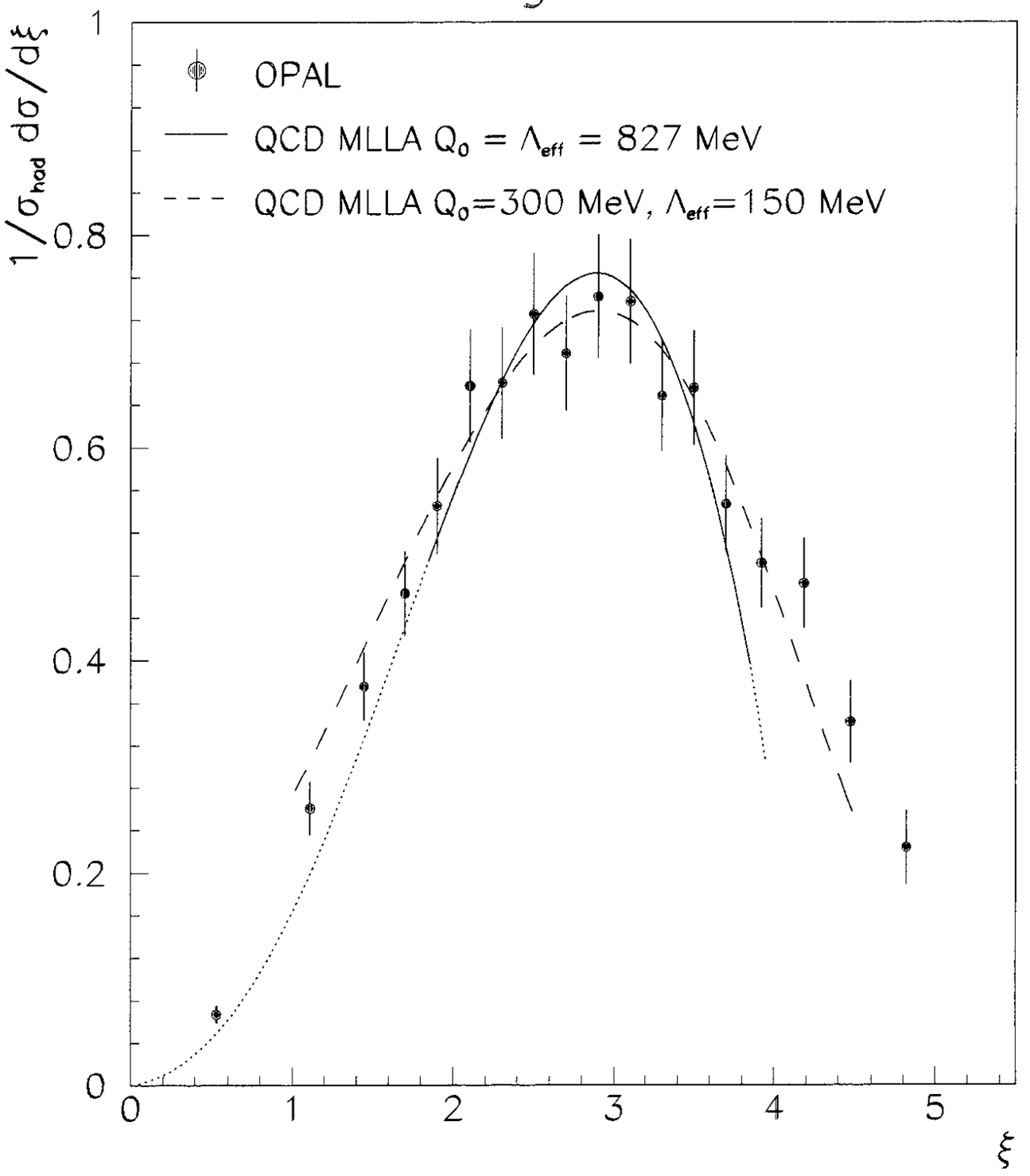
OPAL
QCD MLLA $Q_0 = \Lambda_{eff} = 827$ MeV
QCD MLLA Q_0=300 MeV, Λ_{eff}=150 MeV
$1/\sigma_{had}\, d\sigma/d\xi$
ξ
0
0.2
0.4
0.6
0.8
1
0
1
2
3
4
5

Fig. 4a

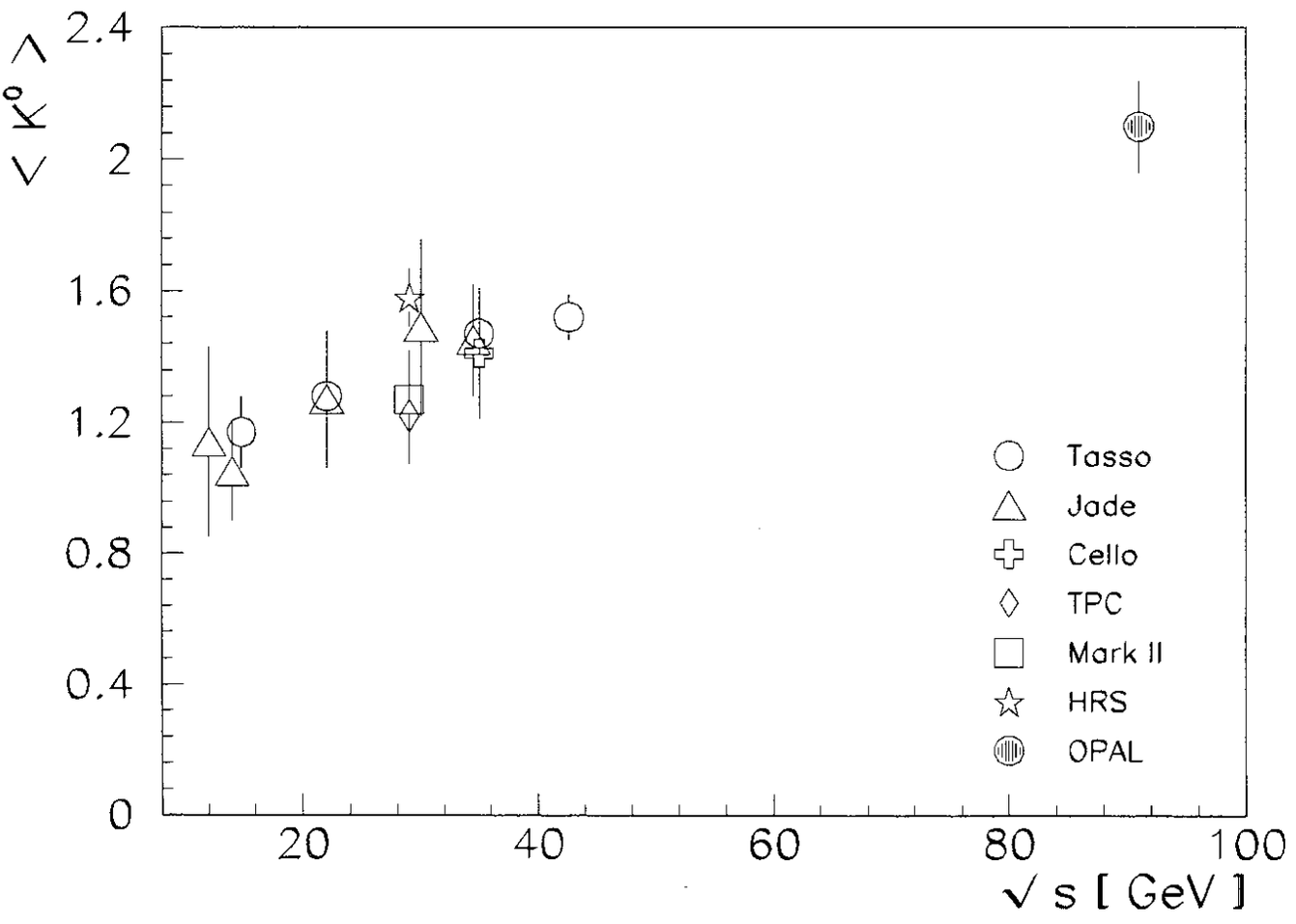
2.4
2
1.6
1.2
0.8
0.4
0
20
40
60
80
100
√ s [GeV]
Tasso
Jade
Cello
TPC
Mark II
HRS
OPAL

Fig. 4b

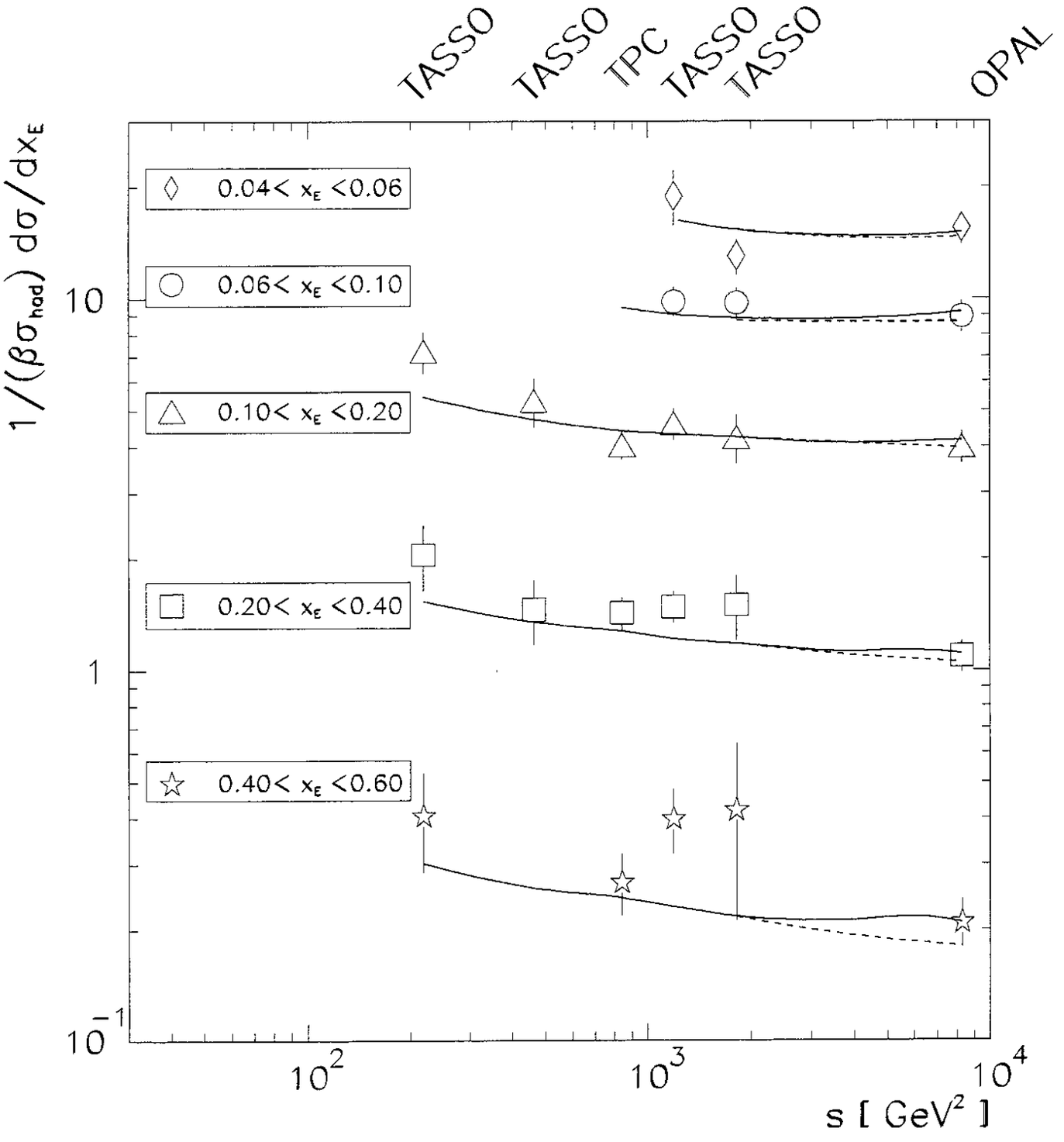
TASSO
TASSO
TPC
TASSO
TASSO
OPAL
$1/(\beta\sigma_{had})\ d\sigma/dx_E$
$0.04< x_E <0.06$
$0.06< x_E <0.10$
$0.10< x_E <0.20$
$0.20< x_E <0.40$
$0.40< x_E <0.60$
10
1
10^{-1}
10^2
10^3
10^4
s [GeV^2]